

Sulfur and sulfur-oxide compounds as potential optically active defects on SWCNTs

Tina N. Mihm,¹ Kasidet Jing Trerayapiwat,² Xinxin Li,^{3,4} Xuedan Ma,^{3,5,6} and Sahar Sharifzadeh^{1,7,8,9, a)}

¹⁾*Department of Electrical and Computer Engineering, Boston University, MA, 02215, USA*

²⁾*Department of Chemistry, Boston University, MA, 02215, USA*

³⁾*Center for Nanoscale Materials, Argonne National Laboratory, Lemont, IL 60439, USA*

⁴⁾*Consortium for Advanced Science and Engineering, University of Chicago, Chicago, IL 60637, USA*

⁵⁾*Materials Science and NanoEngineering, Rice University, Houston, TX, 77251, USA*

⁶⁾*Northwestern Argonne Institute of Science and Engineering, Evanston, IL 60208, USA*

⁷⁾*Department of Chemistry, Boston University, Boston, MA, 02215, USA*

⁸⁾*Materials Science Division, Boston University, Boston, MA, 02215, USA*

⁹⁾*Department of Physics, Boston University, Boston, MA, 02215, USA*

(Dated: December 24, 2024)

Semiconducting single-walled carbon nanotubes (SWCNT) containing covalent defects are a promising class of optoelectronic materials, demonstrating single photon emission and long-lived spins. The defect introduces new optical transitions due to both symmetry breaking induced band splitting and introduction of in-gap electronic states. We investigate sulfur-oxide containing compounds as a new class of optically active dopants on (6,5) SWCNT. The SWCNT is exposed to sodium dithionite with the resulting compound displaying a red-shifted and bright photoluminescence peak that is characteristic of these covalent defects. Density functional theory calculations are then performed on the adsorbed compounds that may arise (S, SO, SO₂ and SO₃). These calculations indicate that the two smallest molecules strongly bind to the SWCNT with binding energies of $\sim 1.5 - 1.8$ eV and 0.56 eV for S and SO, respectively. Moreover, these adsorbates introduce in-gap electronic states into the bandstructure of the tube consistent with the measured red-shift of (0.1 – 0.3) eV. Our study suggests that sulfur-based compounds are promising new dopants for (6,5) SWCNT with tunable electronic properties.

Doped semiconducting single walled carbon nanotubes (SWCNT) show promise as optical sensors¹ and quantum light emitters² due to their controlled sensitivity to adsorbates and tunable electron fluorescence.^{1,3-5} For this class of materials, covalent defects introduce new optical transitions that modify the optical absorption spectrum and increase the photoluminescence (PL) efficiency.⁴⁻¹¹ As such, defective SWCNT display high purity single photon emission (SPE) with improved quantum yields^{3,4,8,9,11} for incorporation into bioelectronic devices,^{12,13} sensors¹ and quantum devices.^{2,14}

Dopants are typically introduced to the SWCNT through either breaking of one carbon sp² bond and attaching a ligand that creates an sp³ defect site, or through breaking a C double bond and attaching a ligand that preserves the π -conjugation and the sp² hybridization of the tube. These defects can create a deep trap state (~ 100 meV) that localizes the exciton and significantly improves SPE.^{2,3,7,10,15-17} The most common defects are atomic defects, such as hydrogen¹⁸ and oxygen,^{4,7,9,16} and functionalized aryl groups,^{8,10,17,19-22} with both the oxygen and certain aryl dopants demonstrating both sp² and sp³ type binding.^{7,16,21,22} The

atomic defects, particularly oxygen, form at stable locations on the tube, with a red-shift of the photoluminescence (PL) peak and enhanced photon emissions.^{4,7,9,16} However, the resulting electronic properties of atomic defects synthesized thus far are determined only by the defect binding configuration, limiting the ability to modify their electronic properties.¹⁶ On the other hand, aryl groups and carbon chain dopants offer stable defect sites with slightly more tunability through their functional groups.^{2,8,10,17,19} However, the electronic structure of these molecular-based dopants is hard to control when passivated,^{5,23-25} and has been shown to be defect-independent in certain unpassivated aryl groups.²⁶ Given the close similarities between the limitations of atomic and aryl defects, we explore atomic-like defects, which may provide a practical path for creating doped SWCNT for lower cost of materials that can be produced on an industrial scale.

In this Letter, we present an investigation of new sulfur-oxide-based dopants for (6,5) SWCNT. Similar to oxygen, sulfur oxides are easy to obtain as reactants and so we investigate whether these defects can produce optically active states similar to prior sp³ and sp² defects. By introduction of sodium dithionite to solution-phase (6,5) SWCNT, which we expect results in SO₂ adsorption on the surface, we show that a new doped species is

^{a)}Electronic mail: ssharifz@bu.edu

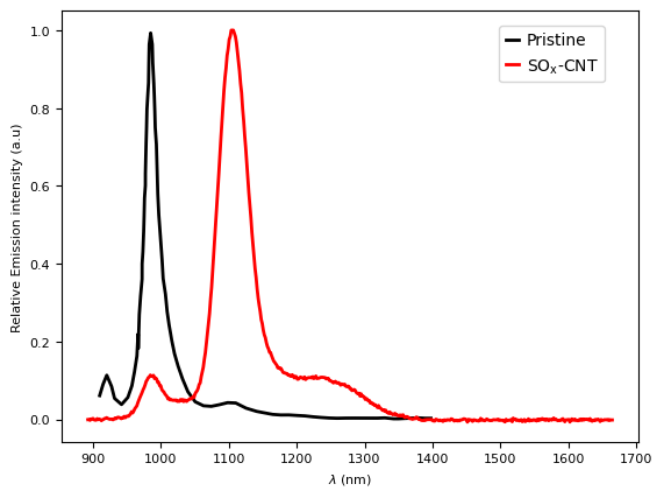


Figure 1. Photoluminescence spectrum of pristine (6,5) SWCNT and (6,5) SWCNT after exposure to sodium dithionite. The data for each plot was normalized such that the maximum intensity is 1 (see SI Fig S.1 for measured spectrum of the doped SWCNT). The pristine spectrum was extracted from Ref 7.

created with the desired red-shifted emissions spectrum as shown in Figure 1. Within density functional theory (DFT), we study the adsorption of sulfur-oxide derivatives that may arise (S, SO, SO₂, SO₃) in order to determine the most likely species that has been synthesized. We predict that the larger two molecules studied, SO₂ and SO₃, are weakly physisorbed to the SWCNT, with little to no electronic interaction to the tube, in agreement with prior DFT-based studies of these compounds on SWCNT.^{27–34} In contrast, S and SO favorably bind to the tube with a red-shifted gap due to either defect-induced band splitting or introduction of an in-gap defect state with S in an sp² bonding configuration being the most energetically stable configuration. Thus, our study indicates that S and SO defects can be incorporated into and tune the optical properties of (6,5) SWCNT.

Figure 1 presents the photoluminescence (PL) spectrum for the SO_x-doped (6,5) SWCNT compared with the pristine tube. The peak maximum is at 1105 nm (1.12 eV) with a low-energy shoulder at 1228 nm (1.0 eV) and another peak at 984 nm (1.26 eV) that is consistent with the pristine tube E₁₁ peak⁷. The fact that new transitions are introduced at 0.1 – 0.3 eV below the pristine gap is consistent with sp² and sp³ doping of the (6,5) SWCNT.^{7,16,19,21,22,35} The details of synthesis and characterization of this system will be published elsewhere. Here, we focus on better understanding the chemical nature and electronic structure of this new species from first-principles DFT simulations.

Figure 2(a) shows the different sulfur compounds considered along with their corresponding binding configuration relative to the SWCNT. We chose S, SO, SO₂, and SO₃ because of prior spectroscopic studies combined with electron microscopy that determined SO₂ may decompose into these compounds on SWCNT.³⁶ We considered different possible configurations of the adsorbate

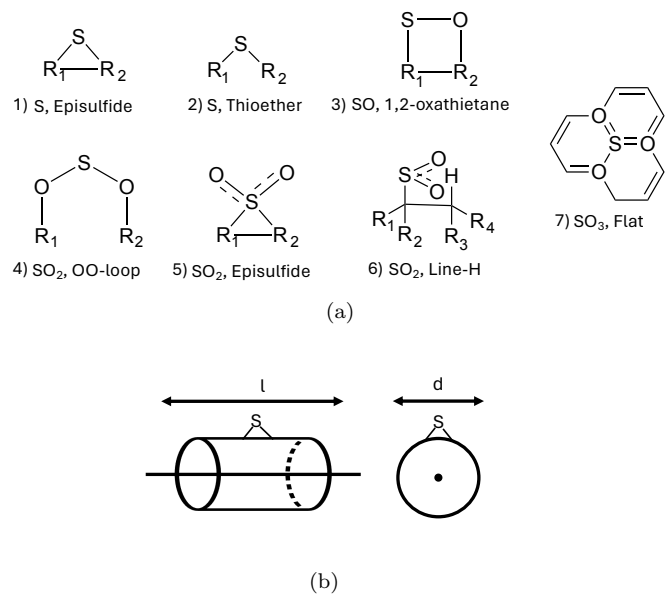


Figure 2. a) The orientation of the different sulfur compounds studied relative to the carbon atoms (R_x) of the SWCNT. b) Illustration of the two different orientations of the sulfur compounds relative to the SWCNT tube axis with a single sulfur atom shown as an example. The cylinder represents the (6,5) SWCNT.

and only show configurations with favorable binding here (see supporting information Section 2.1 for details on unbound structures). For the single sulfur atom, we considered epoxide-type and ether-type binding (structures 1 and 2), both of which have been shown to be energetically favorable locations for oxygen binding on (6,5) SWCNT.¹⁶ For the SO molecule, a four-member ring-type binding (structure 3) with the S and O each bound to one carbon atom was found to be favorable. For each S and SO configuration, we consider two different orientations of the C-S-C bonds, along the long (‘l’) and short (‘d’) axes of the tube (see Fig. 2(b)). For SO₂, three different binding configurations were found to be favorable: 1) the SO₂ attached to two carbons across a broken carbon bond via the two oxygen on the SO₂ labeled “OO-loop” (structure 4), inspired by the orientation of SO₂ bound to graphene sheets;^{37,38} 2) the episulfide-type binding, a modification of the epoxide-type binding of S (structure 5); and 3) with a hydrogen atom attached to a carbon atom neighboring the adsorption site, with the O’s on the SO₂ oriented to be in line with the hydrogen, labeled “Line-H” (structure 6), introduced to test whether H can increase the affinity of the adsorbate to the tube. Lastly, for SO₃, a flat-type binding motivated by binding of SO₃ on graphene is found to be favorable (structure 7).³⁹

We present the binding energies of the sulfur compounds to (6,5) SWCNT in Table I, calculated as,

$$E_b = E_{\text{CNT}+\text{SO}_x} - (E_{\text{CNT}} + E_{\text{SO}_x}). \quad (1)$$

Here, the $E_{\text{CNT}+\text{SO}_x}$ is the total energy of the adsorbate on SWCNT, E_{CNT} is the total energy of the pristine tube,

Table I. Adsorption energy (E_b), band gap (E_{gap}), shift in Fermi energy with respect to the pristine system (ΔE_f), and the energies of the highest valence band (E_{VBM}) and lowest unoccupied state (E_{LUS}) for the defective CNT configurations considered in this work. The adsorption energies are defined such that a negative energy is bound (see Eq. (1)). All energies are in eV.

Structure	E_b	E_{VBM}	E_{LUS}	E_{gap}	ΔE_f
S, Episulfide-l	-1.53	-3.55	-2.91	0.64	0.03
S, Thioether-l	-1.53	-3.55	-2.91	0.64	0.05
S, Episulfide-d	-1.69	-3.60	-2.72	0.88	-0.04
S, Thioether-d	-1.82	-3.61	-2.72	0.89	-0.01
SO, 1,2-oxathietane-l	-0.56	-3.62	-2.78	0.84	-0.07
SO,1,2-oxathietane-d	-0.56	-3.62	-2.78	0.84	-0.07
SO ₂ , OO-loop-d	-0.20	-3.64	-2.72	0.92	-0.04
SO ₂ , Episulfide-d	-0.20	-3.64	-2.73	0.91	-0.05
SO ₂ , Line-H	-0.33	-3.39	-2.73	0.66	0.17
SO ₃ , flat	-0.27	-3.63	-2.75	0.88	-0.08
Pristine	–	-3.62	-2.70	0.92	–

and E_{SO_x} is the total energy of the sulfur compound in vacuum.

The S atom is the most strongly bound to the tube, with binding energy ranging from -1.53 eV to -1.82 eV depending on the bonding arrangement (episulfide or thioether; ‘l’ or ‘d’ orientation). This value is greater than half of a C-S covalent bond energy of ~ 2.7 eV,^{40,41} suggesting strong chemical bonding between the tube and S. For both the thioether-type adsorption, with the S arranged between a broken carbon-carbon bond with sp^2 hybridization, and the episulfide, with the S arranged between a single carbon-carbon bond with sp^3 hybridization, the binding is stronger along the short axis (‘d’) than along the long axis (‘l’) by 0.32 eV for the thioether and 0.16 eV for the episulfide. This finding is consistent with previous studies of oxygen dopants on (6,5) SWCNT,¹⁶ and suggests that the binding of the sulfur on the CNT is influenced by its orientation. In addition, we found that the thioether-l orientation is unstable for the S atom, with the atom reverting to the episulfide, sp^3 hybridized structure upon energy minimization, while thioether-d sp^2 hybridized configuration is more strongly bound than the episulfide-d structure. We note that the thioether-d structure is the only structure studied that retained the sp^2 hybridization of the original SWCNT.

This anisotropy between ‘l’ and ‘d’ directions is not present for the SO molecule, with both orientations predicted to have a binding energy of -0.56 eV. SO₂ and SO₃ display much weaker binding to the surface, more consistent with physisorption. For SO₂, all configurations studied were predicted to bind via physisorption with energies ranging from -0.20 eV (no hydrogen) to -0.33 eV (with hydrogen), indicating that hydrogen only slightly enhances the bond strength. For SO₃, the binding energy is similarly weak at -0.27 eV. That the larger two defects, SO₂ and SO₃, are physisorbed on the surface is consistent with previous studies on carbon nan-

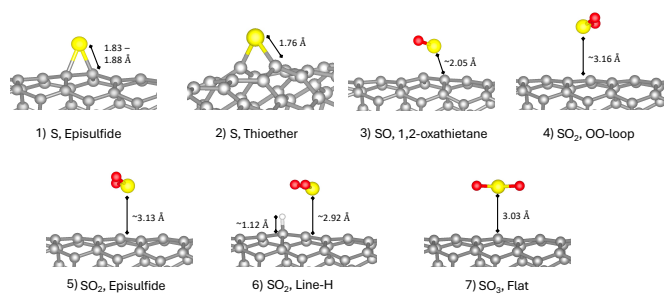


Figure 3. The PBE-D3-predicted adsorption sites of the SO_x structures on (6,5) SWCNT. Relevant bond lengths are labeled.

otubes^{27–33}

We note that there is a slight shift in the Fermi energy of the SWCNT upon doping as shown in Table I. For all but the ‘l’ orientation for sulfur, the Fermi energy shifts slightly towards the VBM, indicating negative charge transfer to the dopant (hole doping). For the sulfur atom in the ‘l’ orientation, the shift is positive, indicating a slight negative charge transfer to the surface. However, the magnitude of all the differences is small, indicating weak doping.

To better understand the binding of SO_x to (6,5) SWCNT, Figure 3 shows the bonding arrangements of select compounds including bond lengths (for all compounds see SI Table S.1). For the sake of comparison, we note that the S-C covalent bond length is ~ 1.8 Å.⁴² For the atomic S adsorbate, the bond length is $1.76 - 1.88$ Å, close to the covalent bond length, with bond angle between the S and tube of $50.2^\circ - 66.4^\circ$ (depending on orientation). The S-C bond is slightly stretched for SO adsorption (~ 2.05 Å) with the bond angles indicating a tilt towards one of the two carbons on the tube (S-R-R angle: $\sim 66^\circ$ and $\sim 71^\circ$), which we attribute to steric effects due to the presence of the oxygen atom. All the SO₂ and the SO₃ structures show an adsorption distance of ~ 3.0 Å away from the SWCNT surface, consistent with the weak binding. For SO₂, the bond angles for the OO-loop-d (S-R-R angle: 82.4° and 72.3°) and Episulfide-d (S-R-R angle: 78.3° and 75.9°) structures indicate the molecule adsorbs slightly off of the C-C bond with S in the hollow site, while the hydrogen passivated structure shows the S in the SO₂ adsorbs on top of a carbon atom (S-R-R angle: 61.2° and 93.8°). SO₃ bond angles (S-R-R angle: 57.5° and 94.0°) also show adsorption of S on top of one of the carbons.

Next, we consider the impact of S, SO, SO₂, and SO₃ on the electronic structure of (6,5) SWCNT. Based on the predicted bonding for the four sulfur compounds to the tube, we may expect that the S and SO compounds are most likely to occur due to their favorable binding energy and will impact the bandstructure most significantly due to their strong bond with the tube. The band structures of select low-energy configurations for the four compounds are shown in Fig. 4 (see SI Figure S.5 for all band structures) and the band gap is presented in Table I.

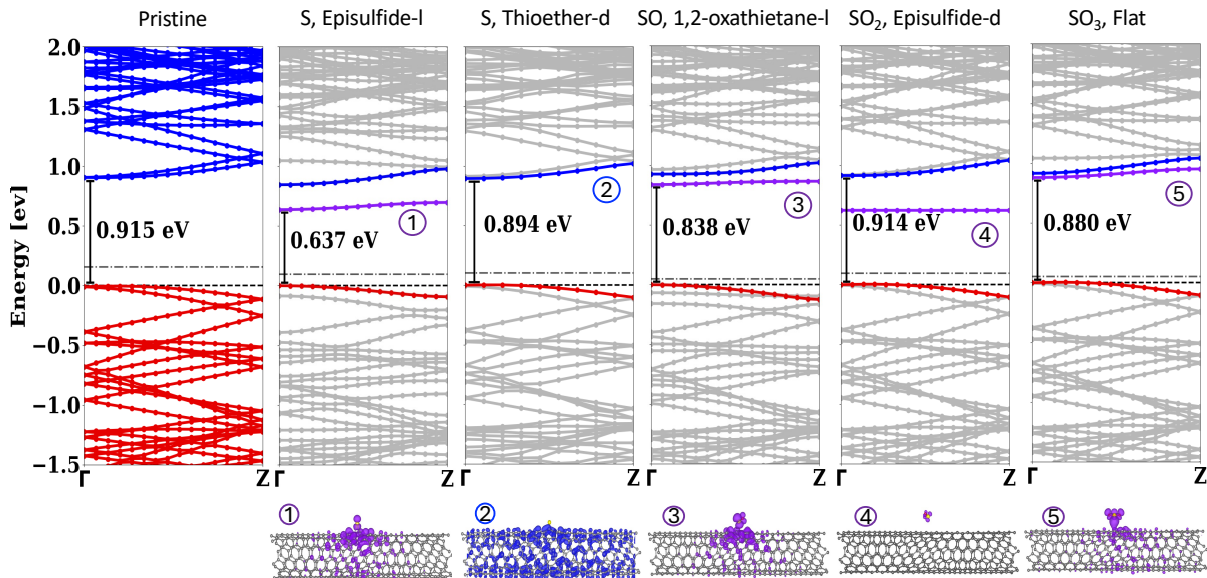


Figure 4. PBE-predicted bandstructure for pristine (6,5) SWCNT and (6,5) SWCNT with the mostly likely adsorbate structures for S, SO, SO₂, and SO₃. Occupied pristine-like valence bands and unoccupied conduction bands are shown in red and blue, respectively, while unoccupied states localized on the defect are in purple. The gray dash-dot line on each band structure represents the Fermi energy. All plots are shifted such that the top of the pristine-like valence band is at zero at $\mathbf{k} = 0$ (indicated by black dash line). The orbital charge density for the lowest energy unoccupied band is shown below the plots with an isosurface that captures 40% of the density.

The near-gap states of the (6,5) SWCNT are of π -type character with a two-fold degeneracy at $\mathbf{k} = 0$ due to the underlying graphitic structure. All the defects presented break the symmetry of the tube, leading to splitting of the nearly-degenerate valence and conduction bands, as has been reported previously for doped (6,5) SWCNT^{5,7-9,16,18,19,35}. This splitting is largest for S, episulfide-l and SO (see SI Figure S.4 for more details) as expected from the stronger binding and therefore stronger perturbation to the system. The maximum splitting of the conduction (valence) bands for episulfide-l S, thioether-d S, and SO are 0.20 eV (0.11 eV), 19 meV (9 meV) and 0.038 eV (0.067 eV), respectively. As noted previously for the oxygen dopant bound to SWCNT,⁷ the ether-type bond between S and the SWCNT maintains the sp^2 character of the tube so the perturbation to the system is weaker than epoxide-type bonding, which creates an sp^3 bond on the tube. This weaker perturbation results in much smaller band splitting. The splitting of the bands for SO₂ is less than 4 meV for both valence and conduction bands, while for SO₃ it is 4 meV for the valence and 0.13 eV for the conduction band.

In addition to symmetry breaking-induced band splitting, both S and SO oriented with the ‘l’ orientation introduce a new unoccupied in-gap state associated with the defect into bandstructure, reducing the gap by up to 0.28 eV for S and 0.08 eV for SO. This in-gap state is associated with a localized defect-centered orbital hybridized with the SWCNT bands as shown in the orbital density plots below the bandstructure. This state is not present for S in the thioether-d configuration for which no

defect-centered orbital is present near the gap. SO₂ also introduces an in-gap state; however, this is a flat band with an associated orbital density that is localized on the defect, indicating no interaction with the tube. For SO₃, there is an in-gap state resonant with the conduction bands. This state is slightly delocalized over parts of the tube and slightly dispersive. However, we suspect that this mixing between the defect state and conduction may be artificial and due to DFT self-interaction error which results in mixing of two resonant states, as occurs in bond dissociation.⁴³ Thus, we predict that only S and SO can introduce new states into the bandstructure of (6,5) SWCNT, leading to a reduced band gap that varies with the defect.

In summary, we studied four possible SO_x defects (S, SO, SO₂, and SO₃) adsorbed onto (6,5) SWCNT in order to understand their adsorption characteristics and impact on the tube electronic structure. We determined that the two smaller defects, S and SO are strongly bound, with bond lengths consistent with a covalent bond with S, and that there is a strong dependence on the directionality along the tube for the bonds formed by S. Furthermore, based on the binding energies to (6,5) SWCNT, we determine that a mixture of S and SO dopants are responsible for the red-shifted peaks in the PL spectrum of Figure 1. S in the sp^2 hybridized thioether-d position is the most strongly bound at 1.8 eV and therefore most likely to form, reducing the gap by ~ 30 meV, slightly smaller than the red-shift of the bright peak in experiment. S in the sp^3 hybridized episulfide-l is also strongly bound and red-shifts the bandgap by 0.3

eV, consistent with the observed low-energy shoulder in the PL spectrum. SO is also strongly bound to the CNT by 0.56 eV and red-shifts the gap by 80 meV, consistent with the brightest peak in the PL spectrum. Our analysis indicates that both S and SO have potential for use as an emissive defect for use in tuning the photoluminescence energy of the SWCNT.

I. EXPERIMENTAL AND COMPUTATIONAL METHODS

A. Computational details

The electronic structure and adsorption energy of the pristine and doped SWCNT were computed within density functional theory (DFT) as implemented in the Vienna Ab initio Simulation Package (VASP)^{44–48}, with frozen-core projector-augmented wave (PAW) pseudopotentials describing the nuclei and core electrons.^{49,50} The exchange-correlation was treated within the generalized gradient approximation (GGA) of Perdew, Burke, and Ernzerhof (PBE)⁵¹, with the addition of Grimme D3 van der Waals corrections.⁵² The choice of the PBE functional was made because empirical van der Waals corrections are better suited to PBE, which tends to underbind, rather than LDA which tends to overbind.^{53,54} All SWCNT were placed in a cubic unit cell with 10 Å of vacuum along the two aperiodic directions. Restricted DFT calculations were performed for all but the ‘In-Line-H’ SO₂ system (See Fig. 2(a)), which requires spin-polarized unrestricted DFT. Calculations were performed with a Γ -centered $1 \times 1 \times 2$ k-point mesh with a plane wave energy cutoff of 400 eV. The structure of the full tube and defect were optimized until all forces were less than 0.01 eV/Å. All energies were converged to less than 1×10^{-6} eV. The optimized lattice vector of the pristine (6,5) SWCNT is $a = 32.4$ Å, $b = 20.0$ Å, and $c = 40.4$ Å and was kept constant in the periodic direction (c) for all the defective systems.

Surface binding energies were computed for the bound (E_{CNT+SO_x}) and isolated (E_{CNT} , E_{SO_x}) systems as defined in Eq. 1. To obtain the total energy of each system, all three systems were placed in the same cell and all the same computational parameters were applied with the exception of the k-mesh for the SO_x calculation, which was $1 \times 1 \times 1$. For the hydrogen passivated SO₂ structure (structure 6 in Fig. 2(a)), we subtract out the binding energy associated with the hydrogen atom (−1.41 eV), which we determined does not interact with SO₂, from the total binding energy ($E_b^{SO_2+H} = -1.74$ eV). Thus, $E_b^{SO_2} = -1.74 + 1.41$ eV.

We note that the experimental SWCNT were suspended in solution using SDS. These long carbon-chain surfactants have been shown to interact with large aryl diazonium defects, with a noticeable impact on the selectivity of the dopant’s binding configuration.^{55,56} However, we expect this impact will be less significant for our

atomic-scale defects, and so we do not account for the surfactant in our binding study. This approximation is consistent with previous studies of oxygen and SO₂/SO₃ defects on SWCNT.^{16,27–34}

B. Experimental Details

Chirality-sorted (6,5) SWCNTs were prepared using a two-step phase separation method, as previously described,^{57,58} and transferred into a 1 wt% sodium dodecyl sulfate (SDS) solution via pressure filtration. The samples were subsequently diluted to an optical density of approximately 0.1 at the E₁₁ absorption peak of the (6,5) SWCNTs by 0.5 wt% SDS solutions. Functionalization of the SWCNTs was carried out using a mixture of sodium bicarbonate and sodium dithionite. The functionalized solution was then stored in the dark for further optical characterizations.

Absorption spectra were measured using a Varian Cary 50 UV-Vis spectrophotometer. Photoluminescence spectra were obtained with a Nanolog spectrofluorometer (Horiba Jobin Yvon), which is equipped with a liquid nitrogen-cooled InGaAs detector.

REFERENCES

- ¹P. W. Barone, S. Baik, D. A. Heller, and M. S. Strano, “Near-infrared optical sensors based on single-walled carbon nanotubes,” *Nature Materials* **4**, 86–92 (2005).
- ²X. He, H. Htoon, S. K. Doorn, W. H. P. Pernice, F. Pyatkov, R. Krupke, A. Jeantet, Y. Chassagneux, and C. Voisin, “Carbon nanotubes as emerging quantum-light sources,” *Nature Materials* **17**, 663–670 (2018).
- ³Q. H. Wang and M. S. Strano, “A bright future for defects,” *Nature Chemistry* **5**, 812–813 (2013).
- ⁴X. Ma, N. F. Hartmann, J. K. S. Baldwin, S. K. Doorn, and H. Htoon, “Room-temperature single-photon generation from solitary dopants of carbon nanotubes,” *Nature Nanotechnology* **10**, 671–675 (2015).
- ⁵B. M. Weight, A. E. Sifain, B. J. Gifford, D. Kilin, S. Kilina, and S. Tretiak, “Coupling between Emissive Defects on Carbon Nanotubes: Modeling Insights,” *The Journal of Physical Chemistry Letters* **12**, 7846–7853 (2021).
- ⁶X. Wang and T. C. Berkelbach, “Excitons in Solids from Periodic Equation-of-Motion Coupled-Cluster Theory,” *Journal of Chemical Theory and Computation* **16**, 3095–3103 (2020).
- ⁷S. Ghosh, S. M. Bachilo, R. A. Simonette, K. M. Beckingham, and R. B. Weisman, “Oxygen Doping Modifies Near-Infrared Band Gaps in Fluorescent Single-Walled Carbon Nanotubes,” *Science* **330**, 1656–1659 (2010).
- ⁸Y. Piao, B. Meany, L. R. Powell, N. Valley, H. Kwon, G. C. Schatz, and Y. Wang, “Brightening of carbon nanotube photoluminescence through the incorporation of sp³ defects,” *Nature Chemistry* **5**, 840–845 (2013).
- ⁹Y. Miyauchi, M. Iwamura, S. Mouri, T. Kawazoe, M. Ohtsu, and K. Matsuda, “Brightening of excitons in carbon nanotubes on dimensionality modification,” *Nature Photonics* **7**, 715–719 (2013).
- ¹⁰X. He, N. F. Hartmann, X. Ma, Y. Kim, R. Ihly, J. L. Blackburn, W. Gao, J. Kono, Y. Yomogida, A. Hirano, T. Tanaka, H. Kataura, H. Htoon, and S. K. Doorn, “Tunable room-temperature single-photon emission at telecom wavelengths from

- sp³ defects in carbon nanotubes,” *Nature Photonics* **11**, 577–582 (2017).
- ¹¹X. He, L. Sun, B. J. Gifford, S. Tretiak, A. Piryatinski, X. Li, H. Htoon, and S. K. Doorn, “Intrinsic limits of defect-state photoluminescence dynamics in functionalized carbon nanotubes,” *Nanoscale* **11**, 9125–9132 (2019).
 - ¹²J. H. Choi, F. T. Nguyen, P. W. Barone, D. A. Heller, A. E. Moll, D. Patel, S. A. Boppart, and M. S. Strano, “Multimodal Biomedical Imaging with Asymmetric Single-Walled Carbon Nanotube/Iron Oxide Nanoparticle Complexes,” *Nano Letters* **7**, 861–867 (2007).
 - ¹³Z. Liu, S. Tabakman, K. Welsher, and H. Dai, “Carbon nanotubes in biology and medicine: In vitro and in vivo detection, imaging and drug delivery,” *Nano Research* **2**, 85–120 (2009).
 - ¹⁴A. Högele, C. Galland, M. Winger, and A. Imamoğlu, “Photon Antibunching in the Photoluminescence Spectra of a Single Carbon Nanotube,” *Physical Review Letters* **100**, 217401 (2008).
 - ¹⁵S.-H. Lohmann, K. J. Trerayapiwat, J. Niklas, O. G. Poluektov, S. Sharifzadeh, and X. Ma, “sp³-Functionalization of Single-Walled Carbon Nanotubes Creates Localized Spins,” *ACS Nano* **14**, 17675–17682 (2020).
 - ¹⁶X. Ma, L. Adamska, H. Yamaguchi, S. E. Yalcin, S. Tretiak, S. K. Doorn, and H. Htoon, “Electronic Structure and Chemical Nature of Oxygen Dopant States in Carbon Nanotubes,” *ACS Nano* **8**, 10782–10789 (2014).
 - ¹⁷A. Ishii, X. He, N. F. Hartmann, H. Machiya, H. Htoon, S. K. Doorn, and Y. K. Kato, “Enhanced Single-Photon Emission from Carbon-Nanotube Dopant States Coupled to Silicon Microcavities,” *Nano Letters* **18**, 3873–3878 (2018).
 - ¹⁸S. Kilina, J. Ramirez, and S. Tretiak, “Brightening of the Lowest Exciton in Carbon Nanotubes via Chemical Functionalization,” *Nano Letters* **12**, 2306–2312 (2012).
 - ¹⁹N. F. Hartmann, S. E. Yalcin, L. Adamska, E. H. Hároz, X. Ma, S. Tretiak, H. Htoon, and S. K. Doorn, “Photoluminescence imaging of solitary dopant sites in covalently doped single-wall carbon nanotubes,” *Nanoscale* **7**, 20521–20530 (2015).
 - ²⁰B. M. Weight, B. J. Gifford, S. Tretiak, and S. Kilina, “Interplay between Electrostatic Properties of Molecular Adducts and Their Positions at Carbon Nanotubes,” *The Journal of Physical Chemistry C* **125**, 4785–4793 (2021).
 - ²¹A. Setaro, M. Adeli, M. Glaeske, D. Przyrembel, T. Bisswanger, G. Gordeev, F. Maschietto, A. Faghani, B. Paulus, M. Weinelt, R. Arenal, R. Haag, and S. Reich, “Preserving π -conjugation in covalently functionalized carbon nanotubes for optoelectronic applications,” *Nature Communications* **8**, 14281 (2017), publisher: Nature Publishing Group.
 - ²²K. Hayashi, Y. Niidome, T. Shiga, B. Yu, Y. Nakagawa, D. Janas, T. Fujigaya, and T. Shiraki, “Azide modification forming luminescent sp² defects on single-walled carbon nanotubes for near-infrared defect photoluminescence,” *Chemical Communications* **58**, 11422–11425 (2022).
 - ²³J. Ramirez, M. L. Mayo, S. Kilina, and S. Tretiak, “Electronic structure and optical spectra of semiconducting carbon nanotubes functionalized by diazonium salts,” *Chemical Physics Photophysics of carbon nanotubes and nanotube composites*, **413**, 89–101 (2013).
 - ²⁴A. Saha, B. J. Gifford, X. He, G. Ao, M. Zheng, H. Kataura, H. Htoon, S. Kilina, S. Tretiak, and S. K. Doorn, “Narrow-band single-photon emission through selective aryl functionalization of zigzag carbon nanotubes,” *Nature Chemistry* **10**, 1089–1095 (2018).
 - ²⁵B. J. Gifford, A. Saha, B. M. Weight, X. He, G. Ao, M. Zheng, H. Htoon, S. Kilina, S. K. Doorn, and S. Tretiak, “Mod(n,m ,3) Dependence of Defect-State Emission Bands in Aryl-Functionalized Carbon Nanotubes,” *Nano Letters* **19**, 8503–8509 (2019).
 - ²⁶K. J. Trerayapiwat, S. Lohmann, X. Ma, and S. Sharifzadeh, “Tuning spin-orbit coupling in (6,5) single-walled carbon nanotube doped with sp³ defects,” *Journal of Applied Physics* **129**, 014309 (2021).
 - ²⁷Y. Chen, S. Yin, Y. Li, W. Cen, J. Li, and H. Yin, “Curvature dependence of single-walled carbon nanotubes for SO₂ adsorption and oxidation,” *Applied Surface Science* **404**, 364–369 (2017).
 - ²⁸S. Yu and W. Yi, “Single-Walled Carbon Nanotubes as a Chemical Sensor for SO₂ Detection,” *IEEE Transactions on Nanotechnology* **6**, 545–548 (2007), conference Name: IEEE Transactions on Nanotechnology.
 - ²⁹M. Mittal and A. Kumar, “Carbon nanotube (CNT) gas sensors for emissions from fossil fuel burning,” *Sensors and Actuators B: Chemical* **203**, 349–362 (2014).
 - ³⁰F. Yao, D. L. Duong, S. C. Lim, S. B. Yang, H. R. Hwang, W. J. Yu, I. H. Lee, F. Güneş, and Y. H. Lee, “Humidity-assisted selective reactivity between NO₂ and SO₂ gas on carbon nanotubes,” *Journal of Materials Chemistry* **21**, 4502–4508 (2011).
 - ³¹A. Goldoni, R. Larciprete, L. Petaccia, and S. Lizzit, “Single-Wall Carbon Nanotube Interaction with Gases: Sample Contaminants and Environmental Monitoring,” *Journal of the American Chemical Society* **125**, 11329–11333 (2003).
 - ³²S. Peymani, M. Izadyar, and A. Nakhaeipour, “Functionalization of the Single-walled Carbon Nanotubes by Sulfur Dioxide and Electric Field Effect, a Theoretical Study on the Mechanism,” *Physical Chemistry Research* **4**, 553–565 (2016).
 - ³³M. Oftadeh, M. Gholamian, and H. H. Abdallah, “Sulfur Dioxide Internal and External Adsorption on the Single-Walled Carbon Nanotubes: DFT Study,” *Physical Chemistry Research* **2**, 30–40 (2014).
 - ³⁴W. Shen, F. Li, C. Liu, and L.-C. Yin, “The dependence of SO₃ dissociation on the diameter of single-wall carbon nanotubes based on first-principles calculations,” *Chemical Physics Letters* **608**, 1–5 (2014).
 - ³⁵K. J. Trerayapiwat, X. Li, X. Ma, and S. Sharifzadeh, “Broken Symmetry Optical Transitions in (6,5) Single-Walled Carbon Nanotubes Containing sp³ Defects Revealed by First-Principles Theory,” *Nano Letters* **24**, 667–671 (2024).
 - ³⁶A. Goldoni, L. Petaccia, L. Gregoratti, B. Kaulich, A. Barinov, S. Lizzit, A. Laurita, L. Sangaletti, and R. Larciprete, “Spectroscopic characterization of contaminants and interaction with gases in single-walled carbon nanotubes,” *Carbon* **42**, 2099–2112 (2004).
 - ³⁷E. Humeres and R. d. F. P. M. Moreira, “Kinetics and mechanisms in flow systems: reduction of SO₂ on carbons,” *Journal of Physical Organic Chemistry* **25**, 1012–1026 (2012), eprint: <https://onlinelibrary.wiley.com/doi/pdf/10.1002/poc.3001>.
 - ³⁸E. Humeres, N. A. Debacher, R. d. F. P. M. Moreira, J. A. Santaballa, and M. Canle, “Reactive Site Model of the Reduction of SO₂ on Graphite,” *The Journal of Physical Chemistry C* **121**, 14649–14657 (2017).
 - ³⁹A. Shokuhi Rad, M. Esfahanian, S. Maleki, and G. Gharati, “Application of carbon nanostructures toward SO₂ and SO₃ adsorption: a comparison between pristine graphene and N-doped graphene by DFT calculations,” *Journal of Sulfur Chemistry* **37**, 176–188 (2016).
 - ⁴⁰“Covalent Bond Energies,” .
 - ⁴¹“Fundamentals of Chemical Bonding,” (2013).
 - ⁴²W. Haynes, *CRC Handbook of Chemistry and Physics* (CRC Press, 2016).
 - ⁴³A. Ruzsinszky, J. P. Perdew, G. I. Csonka, O. A. Vydrov, and G. E. Scuseria, “Spurious fractional charge on dissociated atoms: Pervasive and resilient self-interaction error of common density functionals,” *The Journal of Chemical Physics* **125**, 194112 (2006).
 - ⁴⁴G. Kresse and J. Furthmüller, “Efficient iterative schemes for ab initio total-energy calculations using a plane-wave basis set,” *Physical Review B* **54**, 11169–11186 (1996).
 - ⁴⁵G. Kresse and J. Furthmüller, “Efficiency of ab-initio total energy calculations for metals and semiconductors using a plane-wave basis set,” *Computational Materials Science* **6**, 15–50 (1996).
 - ⁴⁶G. Kresse and J. Hafner, “Ab initio molecular dynamics for liquid metals,” *Physical Review B* **47**, 558–561 (1993).
 - ⁴⁷G. Kresse and J. Hafner, “Ab initio molecular-dynamics simula-

- tion of the liquid-metal–amorphous-semiconductor transition in germanium,” *Physical Review B* **49**, 14251–14269 (1994).
- ⁴⁸G. Kresse and J. Hafner, “Norm-conserving and ultrasoft pseudopotentials for first-row and transition elements,” *Journal of Physics: Condensed Matter* **6**, 8245–8257 (1994).
- ⁴⁹P. E. Blöchl, “Projector augmented-wave method,” *Physical Review B* **50**, 17953–17979 (1994).
- ⁵⁰G. Kresse and D. Joubert, “From ultrasoft pseudopotentials to the projector augmented-wave method,” *Physical Review B* **59**, 1758–1775 (1999).
- ⁵¹J. P. Perdew, K. Burke, and M. Ernzerhof, “Generalized Gradient Approximation Made Simple,” *Physical Review Letters* **77**, 3865–3868 (1996).
- ⁵²S. Grimme, J. Antony, S. Ehrlich, and H. Krieg, “A consistent and accurate ab initio parametrization of density functional dispersion correction (DFT-D) for the 94 elements H-Pu,” *The Journal of Chemical Physics* **132**, 154104 (2010).
- ⁵³L. He, F. Liu, G. Hautier, M. J. T. Oliveira, M. A. L. Marques, F. D. Vila, J. J. Rehr, G.-M. Rignanese, and A. Zhou, “Accuracy of generalized gradient approximation functionals for density-functional perturbation theory calculations,” *Physical Review B* **89**, 064305 (2014).
- ⁵⁴P. Haas, F. Tran, and P. Blaha, “Calculation of the lattice constant of solids with semilocal functionals,” *Physical Review B* **79**, 085104 (2009).
- ⁵⁵X. He, B. J. Gifford, N. F. Hartmann, R. Ihly, X. Ma, S. V. Kilina, Y. Luo, K. Shayan, S. Strauf, J. L. Blackburn, S. Tretiak, S. K. Doorn, and H. Htoon, “Low-Temperature Single Carbon Nanotube Spectroscopy of sp³ Quantum Defects,” *ACS Nano* **11**, 10785–10796 (2017), publisher: American Chemical Society.
- ⁵⁶A. J. Hilmer, T. P. McNicholas, S. Lin, J. Zhang, Q. H. Wang, J. D. Mendenhall, C. Song, D. A. Heller, P. W. Barone, D. Blankschtein, and M. S. Strano, “Role of Adsorbed Surfactant in the Reaction of Aryl Diazonium Salts with Single-Walled Carbon Nanotubes,” *Langmuir* **28**, 1309–1321 (2012), publisher: American Chemical Society.
- ⁵⁷J.-S. Chen, K. J. Trerayapiwat, L. Sun, M. D. Krzyaniak, M. R. Wasielewski, T. Rajh, S. Sharifzadeh, and X. Ma, “Long-lived electronic spin qubits in single-walled carbon nanotubes,” *Nature Communications* **14**, 848 (2023).
- ⁵⁸J.-S. Chen, A. Dasgupta, D. J. Morrow, R. Emmanuele, T. J. Marks, M. C. Hersam, and X. Ma, “Room Temperature Lasing from Semiconducting Single-Walled Carbon Nanotubes,” *ACS Nano* **16**, 16776–16783 (2022).